8266 *Biochemistry* **2010,** *49,* 8266–8275
DOI: 10.1021/bi100920w

BIOCHEMISTRY
including biophysical chemistry & molecular biology
Article

Binding of the Dimeric *Deinococcus radiodurans* Single-Stranded DNA Binding Protein to Single-Stranded DNA[†]

Alexander G. Kozlov,[‡] Julie M. Eggington,[§] Michael M. Cox,[§] and Timothy M. Lohman*[,‡]

[‡]*Department of Biochemistry and Molecular Biophysics, Washington University School of Medicine, 660 South Euclid Avenue, St. Louis, Missouri 63110, and* [§]*Department of Biochemistry, University of Wisconsin, 433 Babcock Drive, Madison, Wisconsin 53706-1544*

Received June 8, 2010; Revised Manuscript Received August 25, 2010

ABSTRACT: *Deinococcus radiodurans* single-stranded (ss) DNA binding protein (*Dr*SSB) originates from a radiation-resistant bacterium and participates in DNA recombination, replication, and repair. Although it functions as a homodimer, it contains four DNA binding domains (OB-folds) and thus is structurally similar to the *Escherichia coli* SSB (*Eco*SSB) homotetramer. We examined the equilibrium binding of *Dr*SSB to ssDNA for comparison with that of *Eco*SSB. We find that the occluded site size of *Dr*SSB on poly(dT) is ~45 nucleotides under low-salt conditions (<0.02 M NaCl) but increases to 50−55 nucleotides at ≥ 0.2 M NaCl. This suggests that *Dr*SSB undergoes a transition between ssDNA binding modes, which is observed for *Eco*SSB, although the site size difference between modes is not as large as for *Eco*SSB, suggesting that the pathways of ssDNA wrapping differ for these two proteins. The occluded site size corresponds well to the contact site size (52 nucleotides) determined by isothermal titration calorimetry (ITC). Electrophoretic studies of complexes of *Dr*SSB with phage M13 ssDNA indicate the formation of stable, highly cooperative complexes under low-salt conditions. Using ITC, we find that *Dr*SSB binding to oligo(dT)s with lengths close to the determined site size (50−55 nucleotides) is stoichiometric with a ΔH_{obs} of approximately -94 ± 4 kcal/mol, somewhat smaller than that for *Eco*SSB (approximately −130 kcal/mol) under the same conditions. The observed binding enthalpy shows a large sensitivity to NaCl concentration, similar to that observed for *Eco*SSB. With the exception of the less dramatic change in occluded site size, the behavior of *Dr*SSB is similar to that of *Eco*SSB protein (although clear quantitative differences exist). These common features for SSB proteins having multiple DNA binding domains enable versatility of SSB function in vivo.

Single-stranded DNA binding proteins are essential in nearly all organisms and play central roles in all aspects of genome maintenance, including DNA replication, recombination, and repair (*1*−*3*). They bind selectively single-stranded DNA with high affinity and in a manner independent of sequence specificity, protecting ssDNA intermediates from degradation and preventing them from the formation of secondary structure. The other functions of SSB proteins have become recognized only recently and include the regulation of the activity of many other DNA metabolic proteins through direct protein−protein interactions (*4*) and modulation of the accessibility of ssDNA[1] by either different modes of binding (*3*, *5*) or the ability to translocate along ssDNA as shown recently for *Eco*SSB (*6*). Although SSB proteins from different organisms can differ in architecture [for example, the bacteriophage T4 gene 32 protein is a monomer (*7*, *8*), *Eco*SSB protein is a homotetramer (*9*−*11*), and eukaryotic RPA proteins are heterotrimers (*12*, *13*)], they all contain oligonucleotide/oligosaccharide binding folds (OB-fold), which form the primary site for ssDNA binding (*14*, *15*). The number of OB-folds varies significantly in these proteins, from one in T4 gene 32 protein to six in the heterotrimeric RPAs. Most of the bacterial SSBs are homotetramers and contain four OB-folds (one per monomer) (see, for example, refs (*16*−*19*)), with the *Eco*SSB tetramer being the most studied. In contrast to the homotetrameric SSB proteins, SSB proteins from the *Deinococcus*−*Thermus* group function as homodimers; however, each monomer encodes two OB-folds linked by a conserved spacer sequence (*20*−*23*). Therefore, the functional form of these proteins still is composed of four OB-folds, although the sequence differences between the two OB-folds within each dimer impose an asymmetry that is likely to affect its DNA binding properties. Furthermore, these dimers possess only two unstructured C-termini, rather than four, which is the case for the homotetrameric SSB proteins.

*Dr*SSB protein originates from one of the most radiation-resistant organisms known (*24*), *Deinococcus radiodurans*, which is a soil bacterium featuring a D_{37} γ irradiation dose of approximately 6000 Gy, making this organism roughly 200 times more radiation-resistant than *Escherichia coli* (*24*). *Dr*SSB forms a stable homodimer in solution (*22*), and its quantitative estimates in the *D. radiodurans* cell indicate approximately 2500−3000 dimers/cell, independent of the level of irradiation (*25*).

A crystal structure of the full-length *Dr*SSB was determined at 1.8 Å resolution (*23*) and shows that each *Dr*SSB subunit comprises two OB-folds linked by a β-hairpin motif and the protein assembles a four-OB-fold arrangement by means of symmetric dimerization. The C-terminal tail residues 234−301 are missing

[†]This research was supported in part by National Institutes of Health Grants GM30498 to T.M.L. and GM32335 to M.M.C.

*To whom correspondence should be addressed: Department of Biochemistry and Molecular Biophysics, Box 8231, Washington University School of Medicine, 660 S. Euclid Ave., St. Louis, MO 63110. E-mail: lohman@biochem.wustl.edu. Telephone: (314) 362-4393. Fax: (314) 362-7183.

[1]Abbreviations: *Dr*SSB, *Deinococcus radiodurans* single-stranded DNA binding protein; ssDNA, single-stranded DNA; ITC, isothermal titration calorimetry; Tris, tris(hydroxymethyl)aminomethane; EDTA, ethylenediaminetetraacetic acid.

 Published on Web 08/26/2010

from the model because of the lack of electron density, suggesting that the extended C-terminal region of this protein is highly unstructured similar to the C-terminal tails of *Eco*SSB (*11*).

To improve our understanding of the functional consequences arising from these differences, we have examined the binding of *Dr*SSB to a variety of ssDNA forms to compare its DNA binding properties with those of the well-studied homotetrameric *Eco*SSB.

MATERIALS AND METHODS

Reagents and Buffers. Buffers were prepared with reagent grade chemicals and distilled water that was subsequently treated with a Milli Q (Millipore, Bedford, MA) water purification system. Buffer T was 10 mM Tris (pH 8.1), and buffer P was 10 mM phosphate (pH 7.5). All buffers contained 0.1 mM Na_3EDTA and 1 mM BME. The concentrations of NaCl used in the experiments are specified in the text.

DrSSB and ssDNA. *Dr*SSB protein was expressed and purified as described previously (*22*, *26*) and its concentration determined spectrophotometrically in Tris buffer (pH 8.1, 0.2 M NaCl) using an extinction coefficient of 8.2×10^4 M^{-1} cm^{-1} (dimer) (*22*). Single-stranded circular phage M13 mp18 DNA was purchased from New England Biolabs, Inc. (Ipswich, MA). The oligodeoxynucleotides, $(dT)_L$ (L = 30, 35, 40, 45, 50, 55, 60, or 70), were synthesized and purified as described previously (*27*) and were ≥98% pure as judged by denaturing gel electrophoresis and autoradiography samples that were 5′ end-labeled with ^{32}P using polynucleotide kinase. The poly(dT) (Midland Certified Reagent Co., Midland, TX) had an average length of ~1100 nucleotides. Concentrations of nucleic acids were determined spectrophotometrically in buffer T (pH 8.1) and 100 mM NaCl using an extinction coefficient ε_{260} of 8.1×10^3 M^{-1} cm^{-1} (nucleotide) for oligo(dT) and poly(dT) (*8*) and an ε_{259} of 7370 M^{-1} cm^{-1} (nucleotide) for single-stranded M13 ssDNA (*28*).

Fluorescence Titrations. Equilibrium binding of *Dr*SSB protein to oligodeoxynucleotides, $(dT)_L$ and poly(dT), was performed by monitoring quenching of the intrinsic Trp fluorescence of *Dr*SSB upon addition of ssDNA using a PTI QM-2000 spectrofluorometer (Photon Technologies, Inc., Lawrenceville, NJ) [λ_{ex} = 296 nm (2 nm excitation band-pass), and λ_{em} = 345 nm (2−4 nm emission band-pass)] with corrections applied as described previously (*29*, *30*). The binding isotherms shown in Figure 2 for the interaction of $(dT)_L$ (L = 45, 50, or 55) (X, ligand) with *Dr*SSB dimer (M, macromolecule) were analyzed using n identical and independent sites model described by eq 1:

$$Q_{obs} = \frac{Q_{max} n K_{obs} X}{1 + K_{obs} X} \quad (1)$$

where Q_{obs} is the observed fluorescence quenching, Q_{max} is the fluorescence quenching at saturation, and n and K_{obs} are the stoichiometry of binding and equilibrium association constant, respectively. The concentration of free $(dT)_L$, X, was determined from the mass conservation equation (eq 1a):

$$X_{tot} = M + X_{bound} = X + \frac{n K_{obs} X}{1 + K_{obs} X} M_{tot} \quad (1a)$$

The binding isotherms shown in Figure 3 for the interaction of two $(dT)_{25}$ molecules (ligand, X) with *Dr*SSB dimer (macromolecule, M) were analyzed using a two-site sequential binding model and eq 2:

$$Q_{obs} = \frac{Q_1 K_{1,obs} X + Q_2 K_{1,obs} K_{2,obs} X^2}{1 + K_{1,obs} X + K_{1,obs} K_{2,obs} X^2} \quad (2)$$

where Q_{obs} is the observed fluorescence quenching, Q_1 and Q_2 are the fluorescence quenchings corresponding to one and two $(dT)_{25}$ molecules bound, respectively, and $K_{1,obs}$ and $K_{2,obs}$ are the observed stepwise macroscopic association constants for the binding of the first and the second DNA molecule, respectively. The concentration of free DNA, X, was determined from the mass conservation equation (eq 2a):

$$X_{tot} = X + X_{bound} = X + \frac{K_{1,obs} X + 2 K_{1,obs} K_{2,obs} X^2}{1 + K_1 X + K_{1,obs} K_{2,obs} X^2} M_{tot} \quad (2a)$$

In eqs 1 and 2, X_{tot} and M_{tot} are total concentrations of $(dT)_L$ and the protein, respectively. The fitting of the data was performed using the nonlinear regression package in Scientist (MicroMath Scientist Software, St. Louis, MO).

Isothermal Titration Calorimetry (*ITC*). ITC experiments were performed using a VP-ITC titration microcalorimeter (MicroCal Inc., Northampton, MA) (*31*). Generally, experiments were conducted by titration of *Dr*SSB [1−2 μM (dimer) in the cell] with oligo(dT) solutions (10−25 μM in the syringe). The heats of dilution were usually obtained from a reference titration in which the species in the syringe is titrated into the cell containing only buffer solution. All corrections for heats of dilution were applied as described previously (*32*). Oligo(dT) and protein samples were dialyzed extensively versus the buffer containing the indicated salt concentration used in the ITC experiments.

The *Dr*SSB binds one molecule of $(dT)_L$, when L = 35, 40, 45, 50, 55, and 60. The stoichiometry of binding, n, and the values of K_{obs} (where measurable) and ΔH_{obs} were obtained by fitting the ITC titration curves to a model of ligand [X = $(dT)_L$] binding to n identical and independent sites on the macromolecule (M = *Dr*SSB) using eq 3

$$Q_i^{tot} = V_0 \Delta H_{obs} M_{tot} \frac{n K_{obs} X}{1 + K_{obs} X} \quad (3)$$

where Q_i^{tot} is the total heat after the ith injection and V_0 is the volume of the calorimetric cell. The concentration of free ligand (X) was obtained by solving eq 1a. When the length of $(dT)_L$ is shorter than 35 nucleotides or longer than 60 nucleotides, the observed binding isotherms display two-step behavior indicative of weak binding of a second $(dT)_L$ molecule (X) to *Dr*SSB (M) (when L < 35) or a second *Dr*SSB dimer (X) to $(dT)_L$ (macromolecule M) (when L > 60). For these cases, we used a two-site sequential binding model, characterized by two macroscopic binding constants ($K_{1,obs}$ and $K_{2,obs}$) and two binding enthalpies ($\Delta H_{1,obs}$ and $\Delta H_{2,obs}$) as described by eq 4

$$Q_i^{tot} = V_0 \Delta H_{obs} M_{tot} \left[\frac{K_{1,obs} X \Delta H_{1,obs} + K_{1,obs} K_{2,obs} X^2 (\Delta H_{1,obs} + \Delta H_{2,obs})}{1 + K_{1,obs} X + K_{1,obs} K_{2,obs} X^2} \right] \quad (4)$$

where the concentration of free ligand (X) was obtained by solving eq 2a. In eqs 3 and 4, X_{tot} and M_{tot} are the total concentrations of the ligand and macromolecule, respectively, in the calorimetric cell after the ith injection. Nonlinear least-squares fitting of the data was performed using the "ITC Data Analysis in Origin" software provided by the manufacturer. The conversion of integral heats (Q_i^{tot}) to differential heats (heats per

injection observed in the experiment) and the fitting routine including corrections for heat displacement effects and ligand and macromolecule dilutions in the calorimetric cell were performed as described previously (*32*) [see also the *ITC Data Analysis in Origin Tutorial Guide* (Microcal Inc.)]. Additional fittings and simulations were also performed using the nonlinear regression package in Scientist (MicroMath Scientist Software).

Agarose Gel Electrophoresis of DrSSB−ssM13 DNA Complexes. The distribution of *Dr*SSB molecules bound to circular phage M13 ssDNA was monitored by separation of the DNA molecules by gel electrophoresis based on the amount of *Dr*SSB bound using 0.5% agarose gels as described previously (*33*). In these experiments, the amount of DNA loaded into each lane was held constant at ≈1.5 nmol (nucleotides) while the amount of *Dr*SSB in the solution was varied from 0 to 0.03 nmol (dimer) to saturate the M13mp8 with *Dr*SSB, assuming that the *Dr*SSB binding site size is 45−50 nucleotides. The complexes were formed in buffer T [10 mM Tris (pH 8.1) and 0.1 mM EDTA] at two NaCl concentrations (0.02 and 0.3 M); the total reaction volume of each sample was 30 μL. The time of incubation was varied as noted in the text. The electrophoresis running buffer consisted of 20 mM Tris-acetate (pH 8.1) and 0.5 mM Na_3EDTA. Loading dye [2 μL of 50% (v/v) glycerol and 0.04% (w/v) bromophenol blue] was added to each 30 μL sample. Electrophoresis was conducted at room temperature (22 °C) at constant voltage (8 V/cm) for ~3 h. The gels were then stained for 15 min with ethidium bromide (2 μg/mL solution) and destained for 2 h at 4 °C in buffer T with 1 M NaCl.

RESULTS

Occluded ssDNA Binding Site Size of DrSSB on Poly(dT). Characterization of the ssDNA binding properties of a nonspecific ssDNA binding protein such as *Dr*SSB requires a determination of the occluded site size (*n*), defined as the number of ssDNA nucleotides that are occluded by one protein and thus prevented from interacting with a second protein (*34*). For oligomeric SSB proteins containing multiple OB-folds and thus potential sites for ssDNA binding, the occluded site size will be affected by the number of OB-folds that are involved in the interaction. For example, the *Eco*SSB homotetramer, possessing four OB-folds (one per subunit), can bind ssDNA in multiple binding modes. Two of the major binding modes differ in that ssDNA occupies two and four subunits with corresponding occluded site sizes of ~35 and 65 nucleotides, respectively (*3*, *35*). Both modes involve at least partial wrapping of ssDNA around the tetramer (*10*). The relative populations of these binding modes are influenced by protein binding density, salt type and valence, and salt concentration (*5*, *35*−*39*), with the SSB_{35} binding mode preferred under low-salt conditions (< 0.02 M NaCl) and high protein binding densities and the SSB_{65} binding mode favored under high-salt conditions (≥ 0.2 M NaCl). Similar effects have been observed for the *Saccharomyces cerevisiae* RPA (scRPA) where the occluded site size increases from ~18 nucleotides under low-salt conditions to ~27 nucleotides under high-salt conditions as a result of the interaction of ssDNA with an additional OB-fold within the scRPA heterotrimer (*40*).

We measured the occluded site size for the *Dr*SSB dimer binding to the homopolynucleotide poly(dT) as a function of salt concentration to determine if multiple ssDNA binding modes could be detected for this protein. The results of *Dr*SSB titrations with poly(dT) at different NaCl concentrations (Tris buffer, pH 8.1, 25 °C), monitoring the quenching of *Dr*SSB tryptophan fluorescence, are presented in Figure 1 and Table 1. In the absence of added salt and at a low NaCl concentration (20 mM) (see Figure 1A), the Trp fluorescence quenching increases linearly with increasing poly(dT) concentration, reaching a quenching plateau of 72% (no salt added) and 76% (20 mM NaCl) at saturating poly(dT). The intersection of the initial linear region with the plateau occurs at ≈45 nucleotides per *Dr*SSB dimer, providing an estimate of the occluded site size of the *Dr*SSB dimer on poly(dT). The observed stoichiometries were independent of *Dr*SSB concentration (titrations performed at 70 and 200 nM *Dr*SSB), indicating that binding is stoichiometric under these conditions. Similar stoichiometric binding is observed at 0.2 and 0.5 M NaCl (see Figure 1B); however, both the occluded site size and the maximum Trp fluorescence quenching increase to ≈50−55 and 83−84%, respectively. Titrations performed at a still higher NaCl concentration of 1 M results in a binding isotherm indicating that binding is no longer stoichiometric (Figure 1B), making it impossible to determine an occluded site size by the extrapolation method. Thus, binding at 1 M NaCl is no longer stoichiometric. This is different from what is observed

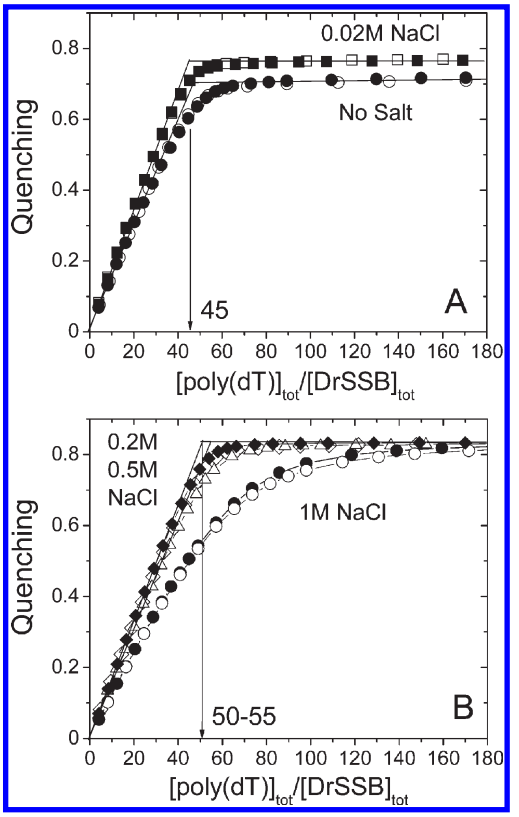

FIGURE 1: Determination of the occluded site size of *Dr*SSB on poly(dT) at different NaCl concentrations (buffer T, pH 8.1, 25 °C). (A) Results of fluorescence titrations of *Dr*SSB [0.07 μM (□) and 0.2 μM (■)] with poly(dT) in 0.02 M NaCl and in the absence of salt [0.07 μM (○) and 0.2 μM (●)]. (B) Results of fluorescence titrations of *Dr*SSB with poly(dT) in 0.2 M NaCl [0.07 μM (◇) and 0.2 μM (◆)], 0.5 M NaCl [0.1 μM (△)], and 1.0 M NaCl [0.1 μM (○) and 0.2 μM (●)]. The linear increase in relative quenching indicates stoichiometric binding of the protein to poly(dT) until the point of saturation (plateau value) is reached. The occluded site sizes were determined by extrapolation of the linear parts of the titration curves to the point of intersection with the corresponding plateau value as described previously (*35*) and yield ≈45 nucleotides per *Dr*SSB dimer (A) and ≈50−55 nucleotides per *Dr*SSB dimer (B). For 1 M NaCl, the binding is not stoichiometric, so a determination of the occluded site size is not posssible.

Table 1: Results of Equilibrium Titrations of *Dr*SSB with ssDNA Monitoring Trp Fluorescence Quenching[a]

	poly(dT)			$(dT)_{50}$ (1:1)		$(dT)_{45}$ (1:1)		$(dT)_{25}$ (2:1)	
[NaCl] (M)	n[b] (no. of nucleotides)	Q_{max}	K_{obs}[c] (M^{-1})	Q_{max}	K_{obs}[c] (M^{-1})	Q_{max}	K_{obs}[c] (M^{-1})	Q_1, Q_2	$K_{1,obs}$, $K_{2,obs}$[c] (M^{-1})
0	46	0.72	st	–	–	–	–	–	–
0.02	45	0.76	st	0.84	st	0.76	st	0.48 ± 0.01, 0.83 (fixed)	$(4.5 \pm 6.2) \times 10^9$, $(1.4 \pm 0.1) \times 10^5$
0.2	50	0.84	st	0.83	st	0.76	st	0.51 ± 0.01, 0.83 (fixed)	$(3.1 \pm 0.6) \times 10^7$, $(2.1 \pm 0.3) \times 10^5$
0.5	55	0.83	st	–	–	–	–	–	–
1.0	N/A	0.84	N/A	–	–	0.72	$(1.5 \pm 0.1) \times 10^7$	–	–

[a]Solution conditions: 10 mM Tris (pH 8.1) and 0.1 mM EDTA. [b]Occluded site size as the number of nucleotides determined as described in the text. [c]st, stoichiometric binding; the errors are standard deviations.

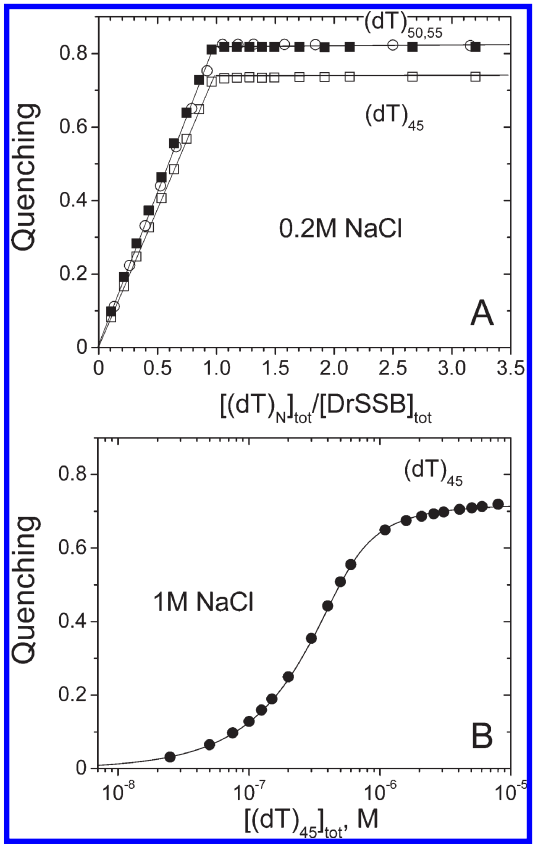

FIGURE 2: Determination of the occluded site size of *Dr*SSB using oligonucleotides of different lengths (buffer T, pH 8.1, 25 °C). (A) Results of fluorescence titrations of *Dr*SSB (~1 μM) with $(dT)_{45}$, $(dT)_{50}$, and $(dT)_{55}$ in the presence of 0.2 M NaCl. (B) Fluorescence titration of *Dr*SSB (~1 μM) with $(dT)_{45}$ in 1.0 M NaCl. The smooth curve represents the best fit of the data using eq 1 (see Materials and Methods) with the following parameters: $n = 0.98 \pm 0.01$, $Q_{max} = 0.72 \pm 0.01$, and $K_{obs} = (1.48 \pm 0.06) \times 10^7$ M^{-1}.

for the binding of *Eco*SSB with poly(dT), where binding remains stoichiometric up to 3 M NaCl and is characterized by an occluded site size of ≈65 with 90−92% quenching (*36*). Hence, *Dr*SSB appears to have a smaller high-salt occluded site size and a lower affinity for poly(dT) compared to *Eco*SSB.

As a further test of whether the high-NaCl concentration site size of the *Dr*SSB dimer on ssDNA exceeds 50−55 nucleotides, we performed titrations of *Dr*SSB with oligodeoxythymidylates of different lengths [$(dT)_L$, where $L = 45$, 50, or 55 nucleotides] at different NaCl concentrations (buffer T, pH 8.1, 25 °C). Figure 2 and Table 1 show the results obtained at 0.2 M NaCl indicating that the *Dr*SSB dimer binds one molecule of $(dT)_{45}$, $(dT)_{50}$, or $(dT)_{55}$, stoichiometrically as expected on the basis of the *Dr*SSB−poly(dT) results. Furthermore, the extent of Trp fluorescence quenching is ~74% for $(dT)_{45}$ but increases to 83−85% for both $(dT)_{50}$ and $(dT)_{55}$, consistent with a high-NaCl concentration site size of ~50 nucleotides. Titrations performed at a lower NaCl concentration [0.02 M NaCl (data not shown)] also show stoichiometric binding behavior with quenching values of ~76% for $(dT)_{45}$ and ~84−85% for $(dT)_{50}$ and $(dT)_{55}$. The results of the titrations of *Dr*SSB with the different $(dT)_L$ oligos suggest that the different behavior observed for *Dr*SSB binding to poly(dT) reflects a real difference in the mode of ssDNA binding, possible reflecting a difference in the mode of ssDNA wrapping and/or interdimer protein−protein cooperativity (see Discussion). It is also clear from the isotherm in Figure 2B that in 1 M NaCl $(dT)_{45}$ interacts with *Dr*SSB much more weakly than at lower NaCl concentrations. The titration curve in Figure 2B can be fitted to an *n*-identical-independent site model (eq 1, Materials and Methods) with the following parameters: $n = 0.98 \pm 0.02$, $Q_{max} = 0.73 \pm 0.01$, and $K = (1.48 \pm 0.06) \times 10^7$ M^{-1}. This suggests that the more shallow isotherm observed in the titration of *Dr*SSB with poly(dT) at 1 M NaCl (Figure 1B) reflects a lower affinity because of the increase in NaCl concentration.

DrSSB Binds Two Molecules of $(dT)_{25}$ with a NaCl Concentration-Dependent Negative Cooperativity. The *Eco*SSB tetramer displays intratetramer negative cooperativity for binding two molecules of $(dT)_{35}$, and this negative cooperativity is a strong function of salt concentration (*41*, *42*). Each subunit of *Dr*SSB dimer contains two OB-folds, and thus, we wanted to determine whether a similar negative cooperativity might exist for ssDNA binding to the *Dr*SSB dimer. Assuming that the full occluded site size for ssDNA binding to the *Dr*SSB dimer is ~50 nucleotides, we examined the equilibrium binding of two molecules of $(dT)_{25}$ to the *Dr*SSB dimer. Panels A and B of Figure 3 show the results of equilibrium titrations of *Dr*SSB with $(dT)_{25}$, monitoring Trp fluorescence at low (0.02 M NaCl) and moderate (0.2 M NaCl) salt concentrations (Tris buffer, pH 8.1, 25 °C), respectively. From these results, it is clear that at both salt concentrations the second molecule of $(dT)_{25}$ binds with weaker affinity than the first molecule, indicating negative cooperativity. Furthermore, the binding of the first $(dT)_{25}$ to *Dr*SSB occurs with a much stronger affinity at the lower NaCl concentration. To estimate the binding parameters, we used a two-site sequential binding model (see eq 2 in Materials and Methods) with two macroscopic binding constants, $K_{1,obs}$ and $K_{2,obs}$ for the first and second sites, with Q_1 and Q_2 characterizing the extents of *Dr*SSB Trp quenching for one and two molecules of $(dT)_{25}$ bound, respectively. For each salt concentration, we globally fit two titration curves by constraining Q_2 to 0.83, corresponding to the maximum fluorescence quenching observed upon binding of

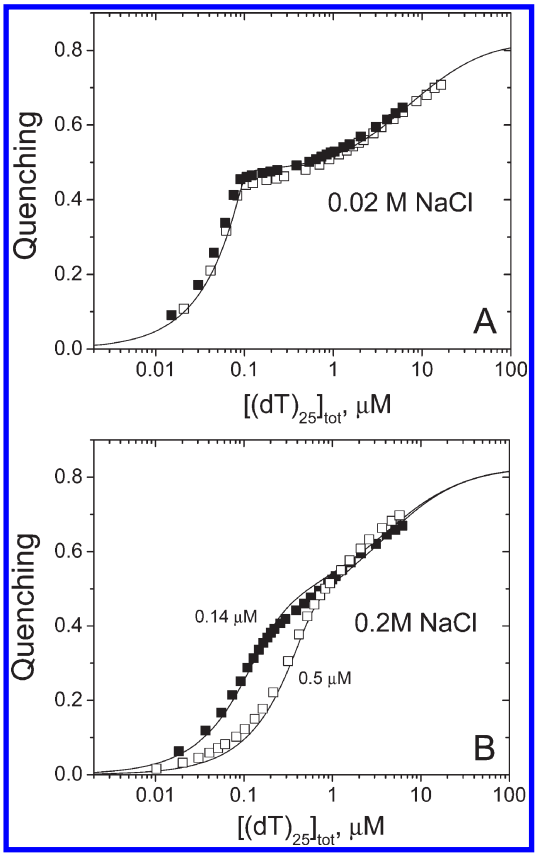

FIGURE 3: *Dr*SSB binds two molecules of $(dT)_{25}$ with negative cooperativity, which decreases with an increase in salt concentration (buffer T, pH 8.1, 25 °C). (A) Two titrations of *Dr*SSB [0.1 μM (□ and ■)] with $(dT)_{25}$ in 0.02 M NaCl. The solid curve represents the result of global nonlinear least-squares fitting of both sets of data to a two-site model (eq 2 in Materials and Methods) with the best fit parameters presented in Table 1. (B) Titration of *Dr*SSB [0.14 μM (■) and 0.5 μM (□)] with $(dT)_{25}$ in 0.2 M NaCl. Solid curves represent the results of global nonlinear least-squares fitting of both sets of data to the two-site model (eq 2 in Materials and Methods) with the best fit parameters presented in Table 1.

poly(dT) and $(dT)_{50}$. The following parameters were obtained: $Q_1 = 0.48 \pm 0.01$, $K_1 = (4.5 \pm 6.2) \times 10^9\ M^{-1}$, and $K_2 = (1.4 \pm 0.1) \times 10^5\ M^{-1}$ for 20 mM NaCl, and $Q_1 = 0.51 \pm 0.01$, $K_1 = (3.1 \pm 0.6) \times 10^7\ M^{-1}$, and $K_2 = (2.1 \pm 0.3) \times 10^5\ M^{-1}$ for 0.2 M NaCl. Interestingly, the affinity for binding of the first $(dT)_{25}$ to *Dr*SSB decreases by a factor of more than 100 as the salt concentration increases 10-fold, whereas the binding of the second $(dT)_{25}$ is essentially unchanged. In general, this observed decrease in negative cooperativity with an increase in NaCl concentration follows the same trend observed for the *Eco*SSB tetramer (*41*, *42*).

Calorimetric Determination of DrSSB Contact Site Size. The contact site size, m, is defined as a number of contiguous nucleotides required to form all interactions with the protein. This may differ from the occluded site size, n, which is a measure of the number nucleotides that are occluded by one protein molecule upon binding to ssDNA, such that the second protein molecule is unable to access these nucleotides; therefore, $m \leq n$. To estimate the contact site size for *Dr*SSB binding to ssDNA, we performed ITC titrations of *Dr*SSB with a $(dT)_L$ series (L = 30, 35, 40, 45, 50, 55, 60, or 70 nucleotides) in 0.2 M NaCl (buffer T, pH 8.1, 25 °C) to determine how the equilibrium binding constant (K_{obs}) and the binding enthalpy (ΔH_{obs}) are affected by L. The magnitude of ΔH_{obs} is expected to increase as

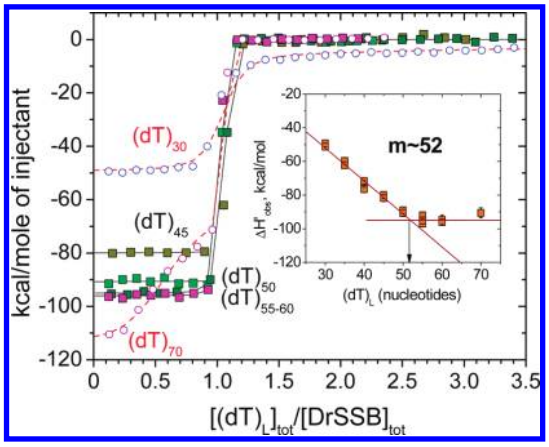

FIGURE 4: Determination of the contact site size of *Dr*SSB and corresponding binding enthalpy using ITC titrations of *Dr*SSB with $(dT)_L$ (L = 30, 35, 40, 45, 50, 55, 60, and 70) in 0.1 M NaCl (buffer T, pH 8.1, 25 °C). The inset shows the decrease in binding ehthalpy with an increase in oligonucleotide length until the number of nucleotides corresponding to the contact site size ($m \approx 52$) is reached. The binding enthalpy ($\Delta H_{obs} = 94 \pm 4$ kcal/mol) was estimated from the plateau value as an average for *Dr*SSB titrations with $(dT)_{55}$, $(dT)_{60}$, and $(dT)_{70}$. In the case of $(dT)_{30}$ and $(dT)_{70}$, the shapes of the isotherms indicate weak binding of the second ssDNA molecule to the *Dr*SSB dimer and the second *Dr*SSB dimer to ssDNA (blue and red open circles, respectively). The reliable estimates for the binding of one ssDNA to one *Dr*SSB dimer ($K_{1,obs}$ and $\Delta H_{1,obs}$) can be obtained for either case by fitting the data to a two-sequential site binding model (eq 4 in Materials and Methods). Dashed curves through experimental data points represents simulations based on the best fit parameters.

the number of nucleotides involved in the protein interaction increases until m is reached.

Figure 4 shows a series of representative ITC isotherms for experiments in which $(dT)_L$ was titrated into *Dr*SSB (0.5–0.8 μM) under the conditions described above. These isotherms indicate that when $40 \leq L \leq 60$ nucleotides, the *Dr*SSB dimer binds one molecule of $(dT)_L$ stoichiometrically, so that the equilibrium binding constant cannot be determined because of the very high affinity ($K_{obs} > 10^9\ M^{-1}$). Under these conditions, only the binding enthalpy (ΔH_{obs}) can be estimated reliably. When L is less than 35, an interaction of a second molecule of $(dT)_L$ with *Dr*SSB can be detected, although this binds with a much weaker affinity (see Figure 4). At the same time, weak binding of a second *Dr*SSB dimer to $(dT)_L$ becomes detectable when the length of oligo(dT) exceeds the binding site size (e.g., see $L \geq 70$ nucleotides in Figure 4). Although in both cases determination of the binding parameters for the second molecule of $(dT)_L$ or *Dr*SSB is not reliable, the estimates of the binding enthalpy for the first molecule ($\Delta H_{1,obs}$) can be obtained accurately. The inset of Figure 4 shows that the values of ΔH_{obs} for the interaction of *Dr*SSB with one molecule of $(dT)_L$ are all negative and increase in magnitude linearly with increasing L up to ≈52 nucleotides, leveling off at $\Delta H_{obs} = 94 \pm 4$ kcal/mol for $L > 50$. These data allow an estimate of $m \approx 52$ nucleotides for the contact site size, which is the same as the estimate of the occluded site size obtained from fluorescence experiments with poly(dT) under the same conditions.

Salt and Temperature Dependencies of the Interaction of DrSSB with $(dT)_{45}$. Solution conditions and salt concentration and type have significant effects on the magnitude of the binding enthalpy (ΔH_{obs}) for the binding of the *Eco*SSB tetramer to ssDNA (*32*, *43*) as well as on its temperature dependence ($\Delta C_{p,obs}$) (*44*).

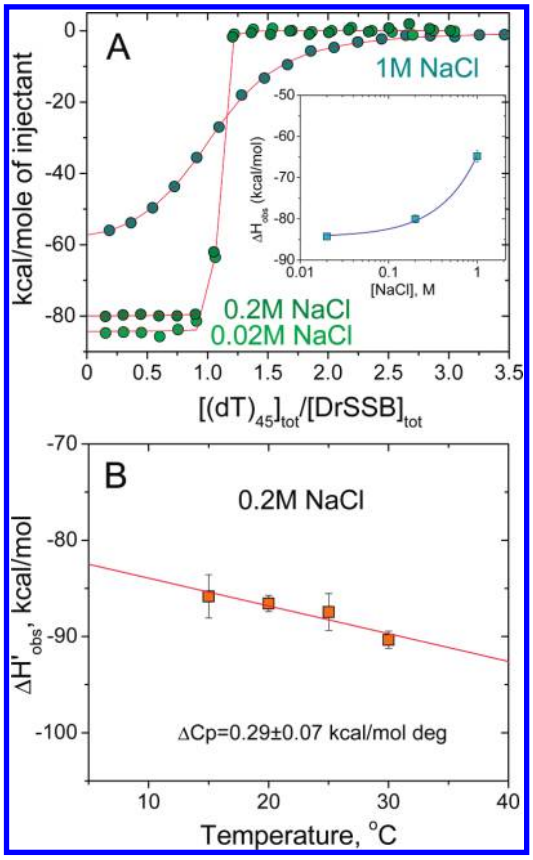

FIGURE 5: Effects of salt concentration and temperature on the observed enthalpy change for *Dr*SSB binding to $(dT)_{45}$. (A) ITC titrations of *Dr*SSB with $(dT)_{45}$ in Tris buffer (pH 8.1) at 0.02 (green), 0.2 (olive), and 1 M NaCl (cyan). Solid curves represent the fits using eq 3 (see Materials and Methods). The binding is stoichiometric at 0.02 and 0.2 M NaCl, so only the values of ΔH_{obs} can be determined, although in 1 M NaCl all binding parameters [$n = 0.99 \pm 0.01$, $K_{obs} = (1.66 \pm 0.14) \times 10^7\ M^{-1}$, and $\Delta H_{obs} = -64.8 \pm 1.4$ kcal/mol] can be estimated. The dependence of ΔH_{obs} on NaCl concentration is shown in the inset. (B) Dependence of ΔH_{obs} on temperature obtained within the range from 15 to 30 °C in phosphate buffer (pH 7.5, 0.2 M NaCl). The $\Delta C_{p,obs}$ value of -0.29 ± 0.07 kcal mol^{-1} deg^{-1} was determined from the linear least-squares fit of the data.

These effects are linked primarily to the release of anions from *Eco*SSB upon ssDNA binding (*44*). To investigate the generality of these effects, we examined the interaction of *Dr*SSB with ssDNA at different NaCl concentrations and temperatures using ITC.

Figure 5A shows the results of 1:1 binding of *Dr*SSB to $(dT)_{45}$ at different NaCl concentrations (buffer T, pH 8.1, 25 °C). The binding is stoichiometric at 0.02 and 0.2 M NaCl but is weakened at 1 M NaCl. Hence, a determination of both ΔH_{obs} and K_{obs} is possible at 1 M NaCl, and the estimated K_{obs} value of $(1.7 \pm 0.1) \times 10^7\ M^{-1}$ is in a good agreement with the value determined by monitoring Trp fluorescence [$K_{obs} = (1.5 \pm 0.1) \times 10^7\ M^{-1}$ (see Figure 2B)]. The ΔH_{obs} values are all negative but exhibit a nonlinear decrease in magnitude as a function of NaCl concentration (see the inset of Figure 5A). This overall dependence of ΔH_{obs} on NaCl concentration is very similar to that observed for *Eco*SSB binding to $(dT)_{70}$ (*32*), indicating a large effect of salt on ΔH_{obs}.

We next examined the temperature dependence of ΔH_{obs} for *Dr*SSB binding to $(dT)_{45}$ in 0.2 M NaCl (buffer P, pH 7.5) (see Figure 5B). Phosphate buffer was used because it has a very low ionization enthalpy and thus minimizes the potential contributions to ΔH_{obs} from any protonation events that may accompany ssDNA binding, which has been observed for *Eco*SSB (*45*). Figure 5B shows that ΔH_{obs} becomes more negative with an increase in temperature. Linear least-squares analysis of the data in Figure 5B yields a $\Delta C_{p,obs}$ value of -290 ± 70 cal mol^{-1} deg^{-1} which is approximately 4 times smaller in magnitude than that measured for the *Eco*SSB−$(dT)_{70}$ interaction under similar conditions (*44*).

Cooperativity of DrSSB Binding to M13 ssDNA Probed by Agarose Gel Electrophoresis. Single-stranded binding proteins have been observed to bind long ssDNA cooperatively under some conditions to form extended protein clusters. The T4 gene 32 protein binds ssDNA with high cooperativity in a manner independent of solution conditions (*7*, *8*). On the other hand, the *Eco*SSB tetramer binds ssDNA with high cooperativity only in its $(SSB)_{35}$ binding mode (*27*, *33*, *37*−*39*, *46*), which is favored at low monovalent salt concentrations and high protein:DNA ratios. In contrast, the fully wrapped $(SSB)_{65}$ binding mode that dominates at high salt concentrations displays little cooperativity (*33*, *37*, *46*−*48*). We were therefore interested in determining whether *Dr*SSB binds to ssDNA with detectable cooperativity and whether salt concentration influences this cooperativity. In general, such information can be described in terms of the intrinsic binding constant (K) and a nearest neighbor cooperativity parameter (ω) using the models of protein binding to infinite (*34*, *49*, *50*) or finite lattices (*51*). Unfortunately, under most conditions (up to 0.5 M NaCl), the binding of *Dr*SSB to poly(dT) is stoichiometric so that accurate determination of the affinity (K) and cooperativity (ω) is not possible. Therefore, to investigate this, we used an agarose gel electrophoresis assay as used in studies of the cooperativity of *Eco*SSB binding to M13 ssDNA (*33*).

We examined the cooperativity of binding of *Dr*SSB to circular M13 ssDNA using an agarose gel electrophoresis assay at two different NaCl concentrations (0.02 and 0.3M). The complexes were formed at varying *Dr*SSB:DNA ratios by directly mixing the *Dr*SSB and M13 ssDNA in buffer T (pH 8.1) and equilibrating for 1 h before electrophoresis (see Materials and Methods). At 0.3 M NaCl (Figure 6A), the ssDNA patterns show a single, somewhat diffuse band at each *Dr*SSB concentration, indicating that all ssDNA molecules have close to the same *Dr*SSB binding density consistent with a low cooperativity of binding of *Dr*SSB to M13 ssDNA. However, at 0.02 M NaCl (Figure 6B), the ssDNA pattern shows a bimodal distribution at intermediate saturation levels (lines 5 and 6, in particular, with 20 and 30% saturation of DNA), indicating of a high degree of cooperativity. These nonrandom binding density distributions at low *Dr*SSB:DNA ratios indicate the presence of ssDNA that has large amounts of *Dr*SSB bound in the same population with ssDNA that has much smaller amounts of *Dr*SSB bound. At higher *Dr*SSB:DNA ratios (≥50% saturation, lanes 8−11), only single bands are observed, indicating a fairly uniform population of highly saturated DNA molecules.

Interestingly, at low protein:DNA ratios (20 and 30% of saturation), the DNA molecules with intermediate binding densities slowly redistribute to form fully saturated DNA and free DNA as indicated by the appearance of corresponding more distinct and sharp bands on the gel (see Figure 6D). Similar experiments performed for the same protein:DNA ratios in 0.3 M NaCl (Figure 6C) show the same random distributions independent of incubation time. Therefore, it appears that *Dr*SSB is able to bind to M13 ssDNA with either very low cooperativity at a high salt concentration (0.3 M NaCl) or much higher cooperativity at

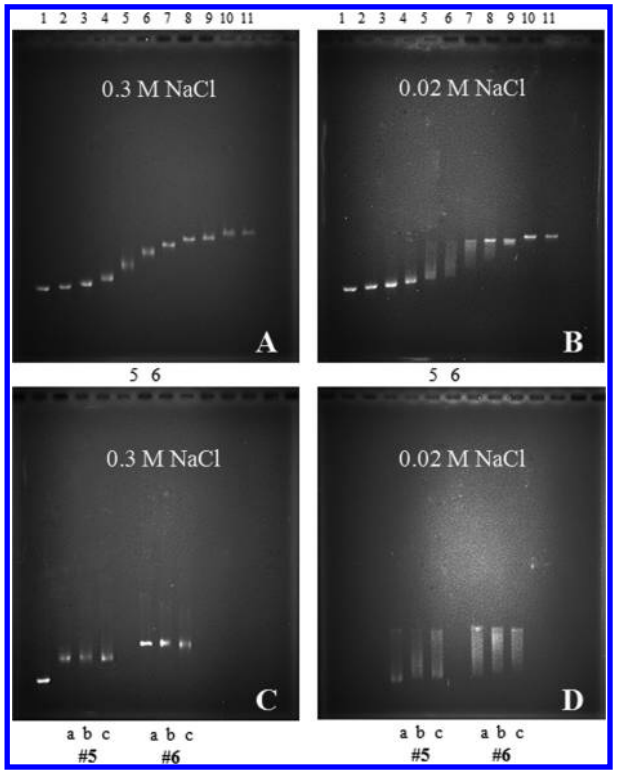

FIGURE 6: Electrophoresis of *Dr*SSB−M13 ssDNA complexes (buffer T, pH 8.1, 22 °C) shows that at low salt concentrations *Dr*SSB forms stable cooperative complexes on ssDNA. The complexes were formed via addition of *Dr*SSB to single-stranded M13mp8 at different protein:ssDNA ratios: $R = 0$ (free DNA) (lane 1), $R = 0.025$ (lane 2), $R = 0.05$ (lane 3), $R = 0.1$ (lane 4), $R = 0.2$ (lane 5), $R = 0.3$ (lane 6), $R = 0.4$ (lane 7), $R = 0.5$ (lane 8), $R = 0.6$ (lane 9), $R = 0.8$ (lane 10), and $R = 1.0$ (lane 11). The ratios $R = n \times$[*Dr*SSB(dimer)/nucleotide] were calculated using site sizes of $n = 45$ and $n = 50$ nucleotides per dimer for 0.02 and 0.3 M NaCl, respectively. (A) In 0.3 M NaCl, gel patterns show only a single band at all protein:DNA ratios, indicative of weak cooperative binding. (B) In 0.02 M NaCl, a nonrandom distribution of protein among the DNA molecules (lanes 4−8) is indicative of cooperative binding. (C) Noncooperative complexes in 0.3 M NaCl [$R = 0.2$ (lane 5), and $R = 0.3$ (lane 6)] after different preincubation times: 18 h (a), 2 h (b), and 10 min (c). (D) Cooperative complexes formed in 0.02 M NaCl (all conditions as described for panel C).

a lower salt concentration (0.02 M). This behavior is similar to that observed for *Eco*SSB. However it is important to point out that in the case of *Eco*SSB the highly cooperative complexes formed at low salt concentrations are metastable and slowly redistribute to random weakly cooperative complexes (*33*), while *Dr*SSB does show the opposite trend, indicative of the high stability of its cooperative complexes.

DISCUSSION

The dimeric *Dr*SSB protein has a four-OB-fold structural organization (two OB-folds per subunit) (*23*) that is similar to that of its *Eco*SSB bacterial analogue. Although the latter forms homotetramers with one OB-fold per subunit (*9*, *10*), they both possess four OB-folds that can provide potential sites for interaction with ssDNA. Structural similarities aside, certain differences observed in the crystal structures of these proteins may affect their interaction with ssDNA. First, *Dr*SSB possesses a structural asymmetry arising from sequence differences between its N- and C-terminal OB domains. In fact, the *Dr*SSB polypeptide sequence of the C-terminal OB-fold is more homologous to the OB-fold in *Eco*SSB than the N-terminal OB-fold (*23*). This raises the possibility that the affinity of the N- and C-terminal OB-folds of *Dr*SSB for ssDNA can differ. Another observation that originates from the analysis of the crystal structure is that the orientation of the two monomers in *Dr*SSB places its OB-folds in positions different from that seen in the *Eco*SSB tetrameric structure. To fit the *Eco*SSB arrangement, one of the *Dr*SSB monomers would need to be rotated to ~40° relative to the other (*23*). Moreover, inspection of the protein−protein interfaces in the crystal structure of *Dr*SSB reveals a large interaction surface linking neighboring dimers through β-hairpin connectors and the N-terminal OB-folds of adjacent molecules (*23*). The latter interactions have been suggested as being potentially responsible for cooperative interactions between *Dr*SSB molecules. However, those interactions are not observed in the *Eco*SSB crystal structures. Therefore, on the basis of the observed differences in crystal structures, it is possible that the ssDNA binding affinities, cooperativities, and modes of ssDNA binding and wrapping may differ for these two proteins and display a different dependence on solution conditions.

DrSSB−ssDNA Binding Mode Transition and Intradimer Negative Cooperativity. At moderate and high salt concentrations (≥0.2 M NaCl), *Eco*SSB forms an $(SSB)_{65}$ binding mode (occluded site size of ~65 nucleotides) in which ssDNA wraps around all four subunits (OB-folds) of the tetramer, whereas at low salt concentrations (≤20 mM NaCl) and high protein:DNA binding ratios, *Eco*SSB binds to ssDNA in a highly cooperative $(SSB)_{35}$ binding mode in which on average only two subunits of the tetramer (two OB-folds) interact with ssDNA (*5*,*27*,*33*,*35*,*36*,*38*,*46*). In this latter mode, ~65−70 nucleotides of ssDNA can accommodate two *Eco*SSB tetramers, which bind with positive cooperativity (*27*).

We show here that *Dr*SSB does undergo a small change in its occluded ssDNA binding site size as a function of NaCl concentration, although the change is not as extreme as the ssDNA binding mode transition observed with *Eco*SSB (*27*, *35*, *36*, *46*). At moderate and high NaCl concentrations (from 0.1 to 1 M), the occluded site size of *Dr*SSB on poly(dT) is 50−53 nucleotides with a Trp fluorescence quenching of ~82%, which agrees well with the contact site size ($m \approx 52$) determined by ITC (Figure 4). However, this is significantly smaller than the high-NaCl concentration induced occluded site size of 65 nucleotides determined for the *Eco*SSB tetramer (>0.2 M NaCl). However, it is interesting to note that the *Eco*SSB tetramer displays a more similar occluded site size of ~56 nucleotides on poly(dT) at intermediate NaCl concentrations (40−100 mM) as well as intermediate $MgCl_2$ concentrations (3−60 mM) (*36*).

At lower NaCl concentrations (≤20 mM), *Dr*SSB displays both a lower extent of Trp fluorescence quenching and a smaller occluded site size ($Q_{max} \approx 0.72-0.76$, and $n \approx 45$) upon binding to poly(dT) as also observed at 1 mM NaCl by Witte et al. (*52*). However, this is still much larger than the low-salt site size of ~35 nucleotides observed for *Eco*SSB (*35*, *36*, *46*). Further evidence that *Dr*SSB dimers do not adopt a very small site size mode at lower NaCl concentrations is the fact that only one *Dr*SSB dimer is observed to bind to oligonucleotides $[(dT)_L]$ with lengths of 45−55 nucleotides. However, the observed difference in site size (45 vs 52 nucleotides) and fluorescence quenching (0.72−0.76 vs 0.83) for the *Dr*SSB dimers binding to ssDNA may result from either a difference in ssDNA wrapping, a difference in cooperative interactions, or both.

The *Dr*SSB binding affinity for ssDNA is strongly dependent on oligodeoxynucleotide length. At moderate salt concentrations, *Dr*SSB binds stoichiometrically to only one molecule of $(dT)_L$ if L is in the range from 40 to 60 nucleotides. For these oligonucleotides, both the Trp fluorescence quenching and enthalpy change increase (in magnitude) with increasing oligonucleotide length up to $n \approx 50-55$ and do not increase further ($Q_{max} \approx 83\%$, and $\Delta H_{obs} \approx -94 \pm 4$ kcal/mol). This can be compared to a Q_{max} of approximately 90% (*41*) and a ΔH_{obs} of approximately −130 kcal/mol (*44*) for *Eco*SSB binding to $(dT)_{65}$. We note that the same extent of Trp fluorescence quenching is observed for *Dr*SSB binding to $(dT)_L$ at both low and high NaCl concentrations (with a maximum of 83−85% quenching for $L >$ 50 nucleotides), whereas a NaCl concentration dependence of Trp quenching is observed for *Dr*SSB binding to poly(dT) (increasing from 72−76 to 84%). This suggests that there are NaCl concentration-dependent effects on *Dr*SSB binding to poly(dT) that are not observed for oligodeoxynucleotide binding. This could reflect effects on the binding mode and/or cooperativity of *Dr*SSB binding to longer ssDNA.

It is also clear from our data that the binding affinity of ssDNA for *Dr*SSB is weaker than for *Eco*SSB. This is emphasized by the fact that the binding constant for oligonucleotides with a length close to its site size is measurable for *Dr*SSB at a NaCl concentration of 1 M, whereas the binding to *Eco*SSB is still stoichiometric up to 3.0 M NaCl (*41*). The binding of a second *Dr*SSB dimer (although with much lower affinity) is detectable only on $(dT)_{70}$ (Figure 4), an oligo that provides 20 additional nucleotides for interaction with the protein, which is in good agreement with results from previous electrophoretic mobility shift assays (*25*). On the other hand, the *Dr*SSB dimer is able to bind a second molecule of ssDNA if it has fewer than 35 nucleotides. Furthermore, the binding of a second molecule of such a shorter oligonucleotide occurs with a significant negative cooperativity that increases with decreasing salt concentration, just as for *Eco*SSB (*41*, *42*, *53*).

DrSSB Forms Stable Highly Cooperative Complexes on ssDNA at Low NaCl Concentrations. Agarose gel electrophoresis has shown that at low salt concentrations (20 mM NaCl) *Eco*SSB can form highly cooperative complexes on ssDNA characterized by nonrandom distributions of *Eco*SSB bound to M13 ssDNA (*33*). However, at a higher NaCl concentration (0.3 M), *Eco*SSB was bound to the ssDNA population in a more random distribution indicative of low cooperative or noncooperative binding. Our experiments with *Dr*SSB performed under the same salt conditions show very similar patterns (Figure 6) indicating that at a low salt concentration (20 mM NaCl) *Dr*SSB binds to ssDNA cooperatively, whereas at higher NaCl concentrations, a low-cooperativity binding distribution is observed. However, in contrast to *Eco*SSB, the *Dr*SSB−ssDNA complexes remain stable and do not redistribute with time to the lower-cooperativity complexes. These results contrast with the sedimentation velocity results of Witte et al. (*52*), who reported that cooperative complexes of *Dr*SSB on poly(dT) are metastable. Analysis of *Dr*SSB crystal structures obtained under different solution conditions reveals a large interaction surface that links neighboring dimers and comprises β-hairpin connectors and N-terminal OB domains of adjacent molecules (*23*). This interface includes a number of van der Waals, hydrogen, and ionic interactions and is different from the L_{45} loop-mediated interface that links *Eco*SSB tetramers (*10*). Although it is still not clear whether the intertetramer interfaces observed in the crystal structures represent the cooperative interactions that exist when bound to ssDNA, these differences raise the possibility that the cooperative complexes formed on ssDNA with *Eco*SSB versus *Dr*SSB may be distinct with different numbers of OB-folds involved in ssDNA wrapping.

Thermodynamics of the Interaction of DrSSB with Oligo(dT). The thermodynamics of *Eco*SSB binding to ssDNA is quite complex and was studied extensively using ITC (*32*, *43*−*45*, *54*). The binding of the *Eco*SSB tetramer to ssDNA is stoichiometric under most of the conditions and is characterized by an extremely large and negative enthalpy change [up to −160 kcal/mol (*32*), the largest enthalpy reported so far for protein−DNA interactions] and a large and negative heat capacity change, $\Delta C_{p,obs}$ [up to −1.2 kcal mol^{-1} K^{-1} (*44*)]. This thermodynamics is explained in large measure by multiple contributions from linked equilibrium reactions that accompany SSB−DNA binding. Among these, the effects of salt concentration and type (*32*, *43*, *44*), protonation (*45*), conformational transitions within DNA (*54*), and protein (*44*) have been quantified.

Using ITC, we find that at moderate salt concentrations (0.2 M NaCl) *Dr*SSB binds to oligodeoxythymidylates with a contact site size of ~52 nucleotides and is characterized by a large and negative ΔH_{obs} of -94 ± 4 kcal/mol, although both of these are significantly smaller than the values measured for *Eco*SSB (approximately −130 kcal/mol and $n = 65$, respectively) under the same conditions (*44*). Interestingly, the values of ΔH_{obs} for these two proteins are similar if normalized by their respective contact sizes (−1.8 and −2.0 kcal/mol per nucleotide). The dependence of ΔH_{obs} on NaCl concentration for *Dr*SSB−$(dT)_{45}$ binding shows nonlinear behavior (Figure 5A), with the largest effect at 1 M NaCl. This behavior is analogous to that observed for *Eco*SSB and related to the contribution to observed enthalpy change due to release of anion from the protein upon interaction with ssDNA (*32*, *44*), which also affects $\Delta C_{p,obs}$ (*44*). The temperature dependence of ΔH_{obs} for *Dr*SSB obtained at 0.2 M NaCl (Figure 5B) provides an estimate of heat capacity change ($\Delta C_{p,obs} = -0.29 \pm 0.07$ kcal mol^{-1} K^{-1}), which is significantly lower than the value of approximately −1.3 kcal mol^{-1} K^{-1} for *Eco*SSB−$(dT)_{70}$ binding under the same conditions (*44*). A large part of the heat capacity change measured for *Eco*SSB is due to contributions from protonation (approximately −0.5 kcal mol^{-1} K^{-1}) and the effects of salt (approximately −0.2 to 0.3 kcal mol^{-1} K^{-1}). The remaining contribution (approximately −0.5 to 0.6 kcal mol^{-1} K^{-1}), which likely reflects changes in accessible surface area upon complexation but may have contributions from protein conformational changes (*44*), is still almost twice as large as the total heat capacity change measured here for *Dr*SSB. In the absence of a more detailed investigation, it is not possible to understand the origins of the lower value of ΔC_p observed for *Dr*SSB, because this could result from a combination of a number of factors such as differences in accessible surface area, vibrational mode hydration, or other coupled equilibria.

ACKNOWLEDGMENT

We thank T. Ho for the synthesis and purification of all oligodeoxynucleotides.

REFERENCES

1. Chase, J. W., and Williams, K. R. (1986) Single-stranded DNA binding proteins required for DNA replication. *Annu. Rev. Biochem. 55*, 103–136.

2. Meyer, R. R., and Laine, P. S. (1990) The single-stranded DNA-binding protein of *Escherichia coli*. *Microbiol. Rev. 54*, 342–380.
3. Lohman, T. M., and Ferrari, M. E. (1994) *Escherichia coli* single-stranded DNA-binding protein: Multiple DNA-binding modes and cooperativities. *Annu. Rev. Biochem. 63*, 527–570.
4. Shereda, R. D., Kozlov, A. G., Lohman, T. M., Cox, M. M., and Keck, J. L. (2008) SSB as an organizer/mobilizer of genome maintenance complexes. *Crit. Rev. Biochem. Mol. Biol. 43*, 289–318.
5. Roy, R., Kozlov, A. G., Lohman, T. M., and Ha, T. (2007) Dynamic structural rearrangements between DNA binding modes of *E. coli* SSB protein. *J. Mol. Biol. 369*, 1244–1257.
6. Roy, R., Kozlov, A. G., Lohman, T. M., and Ha, T. (2009) SSB protein diffusion on single-stranded DNA stimulates RecA filament formation. *Nature 461*, 1092–1097.
7. Alberts, B., Frey, L., and Delius, H. (1972) Isolation and characterization of gene 5 protein of filamentous bacterial viruses. *J. Mol. Biol. 68*, 139–152.
8. Kowalczykowski, S. C., Lonberg, N., Newport, J. W., and von Hippel, P. H. (1981) Interactions of bacteriophage T4-coded gene 32 protein with nucleic acids. I. Characterization of the binding interactions. *J. Mol. Biol. 145*, 75–104.
9. Raghunathan, S., Ricard, C. S., Lohman, T. M., and Waksman, G. (1997) Crystal structure of the homo-tetrameric DNA binding domain of *Escherichia coli* single-stranded DNA-binding protein determined by multiwavelength X-ray diffraction on the selenomethionyl protein at 2.9-Å resolution. *Proc. Natl. Acad. Sci. U.S.A. 94*, 6652–6657.
10. Raghunathan, S., Kozlov, A. G., Lohman, T. M., and Waksman, G. (2000) Structure of the DNA binding domain of *E. coli* SSB bound to ssDNA. *Nat. Struct. Biol. 7*, 648–652.
11. Savvides, S. N., Raghunathan, S., Futterer, K., Kozlov, A. G., Lohman, T. M., and Waksman, G. (2004) The C-terminal domain of full-length *E. coli* SSB is disordered even when bound to DNA. *Protein Sci. 13*, 1942–1947.
12. Wold, M. S. (1997) Replication protein A: A heterotrimeric, single-stranded DNA-binding protein required for eukaryotic DNA metabolism. *Annu. Rev. Biochem. 66*, 61–92.
13. Iftode, C., Daniely, Y., and Borowiec, J. A. (1999) Replication protein A (RPA): The eukaryotic SSB. *Crit. Rev. Biochem. Mol. Biol. 34*, 141–180.
14. Murzin, A. G. (1993) OB(oligonucleotide/oligosaccharide binding)-fold: Common structural and functional solution for non-homologous sequences. *EMBO J. 12*, 861–867.
15. Suck, D. (1997) Common fold, common function, common origin? *Nat. Struct. Biol. 4*, 161–165.
16. Purnapatre, K., Handa, P., Venkatesh, J., and Varshney, U. (1999) Differential effects of single-stranded DNA binding proteins (SSBs) on uracil DNA glycosylases (UDGs) from *Escherichia coli* and mycobacteria. *Nucleic Acids Res. 27*, 3487–3492.
17. Saikrishnan, K., Jeyakanthan, J., Venkatesh, J., Acharya, N., Sekar, K., Varshney, U., and Vijayan, M. (2003) Structure of *Mycobacterium tuberculosis* single-stranded DNA-binding protein. Variability in quaternary structure and its implications. *J. Mol. Biol. 331*, 385–393.
18. Saikrishnan, K., Manjunath, G. P., Singh, P., Jeyakanthan, J., Dauter, Z., Sekar, K., Muniyappa, K., and Vijayan, M. (2005) Structure of *Mycobacterium smegmatis* single-stranded DNA-binding protein and a comparative study involving homologus SSBs: Biological implications of structural plasticity and variability in quaternary association. *Acta Crystallogr. D61*, 1140–1148.
19. Chan, K. W., Lee, Y. J., Wang, C. H., Huang, H., and Sun, Y. J. (2009) Single-stranded DNA-binding protein complex from *Helicobacter pylori* suggests an ssDNA-binding surface. *J. Mol. Biol. 388*, 508–519.
20. Dabrowski, S., Olszewski, M., Piatek, R., Brillowska-Dabrowska, A., Konopa, G., and Kur, J. (2002) Identification and characterization of single-stranded-DNA-binding proteins from *Thermus thermophilus* and *Thermus aquaticus*: New arrangement of binding domains. *Microbiology 148*, 3307–3315.
21. Fedorov, R., Witte, G., Urbanke, C., Manstein, D. J., and Curth, U. (2006) 3D structure of *Thermus aquaticus* single-stranded DNA-binding protein gives insight into the functioning of SSB proteins. *Nucleic Acids Res. 34*, 6708–6717.
22. Eggington, J. M., Haruta, N., Wood, E. A., and Cox, M. M. (2004) The single-stranded DNA-binding protein of *Deinococcus radiodurans*. *BMC Microbiol. 4*, 2.
23. Bernstein, D. A., Eggington, J. M., Killoran, M. P., Misic, A. M., Cox, M. M., and Keck, J. L. (2004) Crystal structure of the *Deinococcus radiodurans* single-stranded DNA-binding protein suggests a mechanism for coping with DNA damage. *Proc. Natl. Acad. Sci. U.S.A. 101*, 8575–8580.
24. Battista, J. R. (1997) Against all odds: The survival strategies of *Deinococcus radiodurans*. *Annu. Rev. Microbiol. 51*, 203–224.
25. Eggington, J. M., Kozlov, A. G., Cox, M. M., and Lohman, T. M. (2006) Polar destabilization of DNA duplexes with single-stranded overhangs by the *Deinococcus radiodurans* SSB protein. *Biochemistry 45*, 14490–14502.
26. Shan, Q., Cox, M. M., and Inman, R. B. (1996) DNA strand exchange promoted by RecA K72R. Two reaction phases with different Mg^{2+} requirements. *J. Biol. Chem. 271*, 5712–5724.
27. Ferrari, M. E., Bujalowski, W., and Lohman, T. M. (1994) Cooperative binding of *Escherichia coli* SSB tetramers to single-stranded DNA in the $(SSB)_{35}$ binding mode. *J. Mol. Biol. 236*, 106–123.
28. Berkowitz, S. A., and Day, L. A. (1974) Molecular weight of single-stranded fd bacteriophage DNA. High speed equilibrium sedimentation and light scattering measurements. *Biochemistry 13*, 4825–4831.
29. Ferrari, M. E., and Lohman, T. M. (1994) Apparent heat capacity change accompanying a nonspecific protein-DNA interaction. *Escherichia coli* SSB tetramer binding to oligodeoxyadenylates. *Biochemistry 33*, 12896–12910.
30. Lohman, T. M., and Mascotti, D. P. (1992) Nonspecific ligand-DNA equilibrium binding parameters determined by fluorescence methods. *Methods Enzymol. 212*, 424–458.
31. Wiseman, T., Williston, S., Brandts, J. F., and Lin, L. N. (1989) Rapid measurement of binding constants and heats of binding using a new titration calorimeter. *Anal. Biochem. 179*, 131–137.
32. Kozlov, A. G., and Lohman, T. M. (1998) Calorimetric studies of *E. coli* SSB protein single-stranded DNA interactions. Effects of monovalent salts on binding enthalpy. *J. Mol. Biol. 278*, 999–1014.
33. Lohman, T. M., Overman, L. B., and Datta, S. (1986) Salt-dependent changes in the DNA binding co-operativity of *Escherichia coli* single strand binding protein. *J. Mol. Biol. 187*, 603–615.
34. McGhee, J. D., and von Hippel, P. H. (1974) Theoretical aspects of DNA-protein interactions: Co-operative and non-co-operative binding of large ligands to a one-dimensional homogeneous lattice. *J. Mol. Biol. 86*, 469–489.
35. Lohman, T. M., and Overman, L. B. (1985) Two binding modes in *Escherichia coli* single strand binding protein-single stranded DNA complexes. Modulation by NaCl concentration. *J. Biol. Chem. 260*, 3594–3603.
36. Bujalowski, W., and Lohman, T. M. (1986) *Escherichia coli* single-strand binding protein forms multiple, distinct complexes with single-stranded DNA. *Biochemistry 25*, 7799–7802.
37. Chrysogelos, S., and Griffith, J. (1982) *Escherichia coli* single-strand binding protein organizes single-stranded DNA in nucleosome-like units. *Proc. Natl. Acad. Sci. U.S.A. 79*, 5803–5807.
38. Griffith, J. D., Harris, L. D., and Register, J., III (1984) Visualization of SSB-ssDNA complexes active in the assembly of stable RecA-DNA filaments. *Cold Spring Harbor Symp. Quant. Biol. 49*, 553–559.
39. Bujalowski, W., Overman, L. B., and Lohman, T. M. (1988) Binding mode transitions of *Escherichia coli* single strand binding protein-single-stranded DNA complexes. Cation, anion, pH, and binding density effects. *J. Biol. Chem. 263*, 4629–4640.
40. Kumaran, S., Kozlov, A. G., and Lohman, T. M. (2006) *Saccharomyces cerevisiae* replication protein A binds to single-stranded DNA in multiple salt-dependent modes. *Biochemistry 45*, 11958–11973.
41. Bujalowski, W., and Lohman, T. M. (1989) Negative co-operativity in *Escherichia coli* single strand binding protein-oligonucleotide interactions. I. Evidence and a quantitative model. *J. Mol. Biol. 207*, 249–268.
42. Bujalowski, W., and Lohman, T. M. (1989) Negative co-operativity in *Escherichia coli* single strand binding protein-oligonucleotide interactions. II. Salt, temperature and oligonucleotide length effects. *J. Mol. Biol. 207*, 269–288.
43. Lohman, T. M., Overman, L. B., Ferrari, M. E., and Kozlov, A. G. (1996) A highly salt-dependent enthalpy change for *Escherichia coli* SSB protein-nucleic acid binding due to ion-protein interactions. *Biochemistry 35*, 5272–5279.
44. Kozlov, A. G., and Lohman, T. M. (2006) Effects of monovalent anions on a temperature-dependent heat capacity change for *Escherichia coli* SSB tetramer binding to single-stranded DNA. *Biochemistry 45*, 5190–5205.
45. Kozlov, A. G., and Lohman, T. M. (2000) Large contributions of coupled protonation equilibria to the observed enthalpy and heat capacity changes for ssDNA binding to *Escherichia coli* SSB protein. *Proteins 4* (Suppl.), 8–22.
46. Lohman, T. M., and Bujalowski, W. (1990) *E. coli* SSB protein: Multiple binding modes and cooperativities. In The Biology of Nonspecific DNA-Protein Interactions (Revzin, A., Ed.) pp 131−170, CRC Press, Boca Raton, FL.

47. Bujalowski, W., and Lohman, T. M. (1987) Limited co-operativity in protein-nucleic acid interactions. A thermodynamic model for the interactions of *Escherichia coli* single strand binding protein with single-stranded nucleic acids in the "beaded", $(SSB)_{65}$ mode. *J. Mol. Biol. 195*, 897–907.
48. Overman, L. B., Bujalowski, W., and Lohman, T. M. (1988) Equilibrium binding of *Escherichia coli* single-strand binding protein to single-stranded nucleic acids in the $(SSB)_{65}$ binding mode. Cation and anion effects and polynucleotide specificity. *Biochemistry 27*, 456–471.
49. Kowalczykowski, S. C., Paul, L. S., Lonberg, N., Newport, J. W., McSwiggen, J. A., and von Hippel, P. H. (1986) Cooperative and noncooperative binding of protein ligands to nucleic acid lattices: Experimental approaches to the determination of thermodynamic parameters. *Biochemistry 25*, 1226–1240.
50. Bujalowski, W., Lohman, T. M., and Anderson, C. F. (1989) On the cooperative binding of large ligands to a one-dimensional homogeneous lattice: The generalized three-state lattice model. *Biopolymers 28*, 1637–1643.
51. Epstein, I. R. (1978) Cooperative and non-cooperative binding of large ligands to a finite one-dimensional lattice. A model for ligand-oligonucleotide interactions. *Biophys. Chem. 8*, 327–339.
52. Witte, G., Urbanke, C., and Curth, U. (2005) Single-stranded DNA-binding protein of *Deinococcus radiodurans*: A biophysical characterization. *Nucleic Acids Res. 33*, 1662–1670.
53. Lohman, T. M., and Bujalowski, W. (1988) Negative cooperativity within individual tetramers of *Escherichia coli* single strand binding protein is responsible for the transition between the $(SSB)_{35}$ and $(SSB)_{56}$ DNA binding modes. *Biochemistry 27*, 2260–2265.
54. Kozlov, A. G., and Lohman, T. M. (1999) Adenine base unstacking dominates the observed enthalpy and heat capacity changes for the *Escherichia coli* SSB tetramer binding to single-stranded oligoadenylates. *Biochemistry 38*, 7388–7397.